EPA-600/R-96-116
September 1996

LARGE BUILDING HVAC SIMULATION

Final Report

by

Lixing Gu, Muthusamy V. Swami, and Vailoor Vasanth

Florida Solar Energy Center
300 State Road 401
Cape Canaveral, FL 32920

DCA Contract 93-RD-66-13-00-22-009
EPA Contract 68-DO-0097, Work Assignment 3-12

EPA Project Officer: Marc Y. Memetrez
National Risk Management Research Laboratory
Research Triangle Park, NC 27711

Prepared for:

State of Florida
Department of Community Affairs
2740 Centerview Drive
Tallahassee, FL 32399

and

U. S. Environmental Protection Agency
Office of Research and Development
Washington, DC 20460

FOREWORD

The U. S. Environmental Protection Agency is charged by Congress with protecting the Nation's land, air, and water resources. Under a mandate of national environmental laws, the Agency strives to formulate and implement actions leading to a compatible balance between human activities and the ability of natural systems to support and nurture life. To meet this mandate, EPA's research program is providing data and technical support for solving environmental problems today and building a science knowledge base necessary to manage our ecological resources wisely, understand how pollutants affect our health, and prevent or reduce environmental risks in the future.

The National Risk Management Research Laboratory is the Agency's center for investigation of technological and management approaches for reducing risks from threats to human health and the environment. The focus of the Laboratory's research program is on methods for the prevention and control of pollution to air, land, water, and subsurface resources; protection of water quality in public water systems; remediation of contaminated sites and groundwater; and prevention and control of indoor air pollution. The goal of this research effort is to catalyze development and implementation of innovative, cost-effective environmental technologies; develop scientific and engineering information needed by EPA to support regulatory and policy decisions; and provide technical support and information transfer to ensure effective implementation of environmental regulations and strategies.

This publication has been produced as part of the Laboratory's strategic long-term research plan. It is published and made available by EPA's Office of Research and Development to assist the user community and to link researchers with their clients.

E. Timothy Oppelt, Director
National Risk Management Research Laboratory

EPA REVIEW NOTICE

ACKNOWLEDGEMENTS

The authors thank the U.S. Environmental Protection Agency (EPA) and contract manager, Marc Menetrez, for funding this work. We also thank the Florida Department of Community Affairs (DCA) and planning manager, Mo Madani, for co-funding the work. The very helpful cooperation of Southern Research Institute (SRI), Bobby E. Pyle, Ashley D. Williamson and Susan E. McDonough is especially acknowledged. Thanks are due to Michael Anello of the Florida Solar Energy Center for his helpful work.

TABLE OF CONTENTS

LIST OF FIGURES

LIST OF TABLES

EXECUTIVE SUMMARY

This report represents work performed by the Florida Solar Energy Center (FSEC) for the Environmental Protection Agency (USEPA-No: 68-D0-0097) and the Florida Department of Community Affairs (DCA-No: 93-RD-66-13-00-22-009). Although individual tasks were funded separately by the two agencies, this report, for the sake of completeness, represents the combined efforts of all simulation related tasks.

Project goals:

The primary goal of the project was to establish the potential for using models to analyze radon levels in large buildings. This was done by applying modelling tools, developed in earlier work and integrated in the computational platform FSEC 3.0, to analyze pressures, airflows and indoor radon levels in a school building monitored by the US EPA and the SRI.

Discussion of effort and results

The effort of the US EPA contract is to simulate pressures, airflows, and radon levels in the Polk Life and Learning Center at Bartow, Florida, monitored by the US EPA and Southern Research Institute (SRI).

First, only the air distribution system of the school building monitored by EPA was simulated to obtain and refine the distribution system parameters. This was done by trial and error while adjusting values of the distribution system parameters and comparing the results with the "test and balancing report" provided by Associated Air Balance Council. After adjustments, the differences between measured and predicted airflows were less than 5%. Next, a steady-state simulation of the soil/slab composite was carried out and the results were compared with experimental data. Because of the nature of the boundary conditions over the slab, a 3-D discretization was required to model the soil/slab composite correctly. Soil/slab parameters were adjusted by trial and error to obtain a reasonable match between predicted and measured values of pressures and airflows. Results of the steady state simulation comparison with measured indoor radon levels agreed to within 6%. Due to paucity of detailed data, it is important to note that the adjusted material properties may not necessarily represent the true values and the calibration may not necessarily translate to other cases.

Keeping the adjusted parameters obtained from earlier runs constant, the next step is to compare measured and calculated indoor radon levels for a transient seven-hour period and a "typical school day" where the system was "on" for the first 12 hours and "off" for the rest of 12 hours. The figure compares histories of predicted and measured indoor radon levels, in one station, for a "typical school day". It is evident that while the agreement at the beginning and end of the "on" cycle is good, the model predicts higher radon dilution rates during the "on" cycle than shown by the experiment. However, the model and experiment compare very well during the "off" period. The disparity noted during "on" times appears consistently in all zones. This is

a significant cause for concern and is possibly due to two factors. 1) The model assumes well mixed zones which may not be true in actuality. The ventilation efficiency may not be 100% leading to different radon levels within a zone and a single-point measurement may be insufficient. 2) The ambient radon level may be higher than assumed. Due to the unavailability of data on ambient radon levels, we assumed a constant of 3.5 pCi/L for simulation purposes. Results of other work for the FRRP (see Tyson et al., 1993) show that ambient radon levels may not only be higher than established action levels, but may also vary cyclically during a 24-hour day. Clearly, the model would predict lower rates of dilution and would approach measured values if higher ambient radon levels are used in the simulation. Undoubtedly, these two factors namely, ventilation efficiency and ambient radon levels, must be investigated further before answering the question definitively.

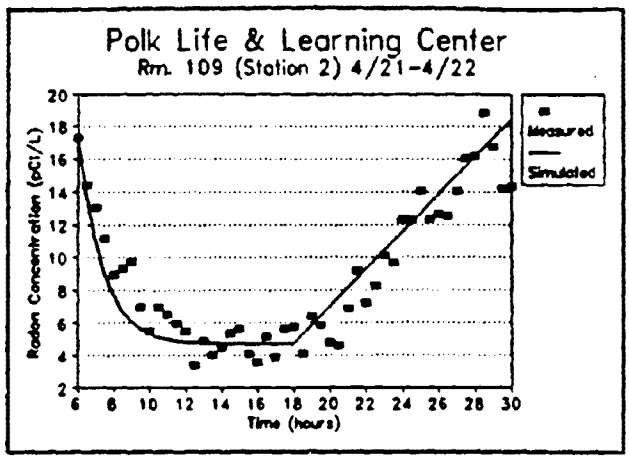

Next, parametric analysis of the effect of varying outdoor airflow, ambient radon level and soil radium content was carried out for this specific building. Indoor radon level decreases with increasing outdoor airflow through the air distribution system, due to dilution. When ambient radon level and soil radium content are varied, there appears to be a linear relationship between indoor radon level and ambient or soil radium content occurs. This determination is specific to the building studied and is based on assumptions stated in the report and may not necessarily translate to other similar buildings.

Caveats:

It is crucial to note that the nature of the work performed here is an exploratory one primarily to establish the potential of using models to analyze large buildings and to identify the essential areas for experiment and simulation to compliment each other in providing an accurate, yet cost efficient strategy to study radon in large buildings. This objective was substantially achieved through a preliminary simulation of airflows and pressures in a school building monitored by the US EPA and the SRI. Since only a limited set of experimental data were available, several assumptions were made to successfully complete the simulations. The results presented in this report, should therefore, be viewed in light of the assumptions stated and applied only to the specific problem analyzed. The result should in no way be construed to represent generalizations for large-buildings. The present report concludes with a list of areas that need further attention.

1. BACKGROUND

1.1 FSEC 3.0 Capabilities

Under support from DCA, Florida Solar Energy Center (FSEC) developed and integrated radon transport in the soil and slab, HVAC system operation, multizone airflow, and zonal contaminant balance into Florida Software for Enervironmetal Computation (FSEC 3.0, 1992). FSEC 3.0 has the following capabilities:

- Zone thermal balance
- Zone moisture balance
- Zone contaminant balance, including radon
- Heat and moisture transport in envelop
- Multizone airflow, including air distribution system
- Several HVAC system models, including VAV box performance
- Duct heat and moisture exchange
- Radon transport in soil and slab
- Detailed air movement in space, used for investigation of ventilation effectiveness

In addition to the above capabilities, FSEC 3.0 offers the following features that make it a promising computational framework for integration of the various models:

- Performs transient or steady 1, 2 or 3-D simulations

- The main computational processor is based on the Galerkin finite element methodology. This lends itself well to irregular shapes and boundary conditions

- Program has already been designed to accommodate up to 250 governing equations. Radon transport equations have been incorporated.

- Several choices for modeling combined heat and mass transport in building are available. This feature is critical to accurately predicting latent loads, indoor conditions and A/C run times in hot humid climates.

- Program allows the user to modify time steps, material properties and boundary conditions on a run-time basis. This is especially important when properties and boundary conditions are functions of space, time, or field variables.

- A building simulator performs the heat and mass balance calculations for the building zones. Subroutine slots are already available to link with other interzone airflow codes.

- Can be run in both PC and VAX/VMS based environments

Many of the capabilities of FSEC 3.0 derive from the software structure itself. The general architecture of the software is given in Figure 1-1. The Computational Processor Segment (CPS) is the heart of the software. It performs the following major operations:

- Computes the capacitance, stiffness and Jacobian matrices and force vectors on an element basis, using numerical volume and surface integrations.

- Assembles the element matrices and force vectors.

- Solves the resulting linear or nonlinear algebraic equations.

This portion of the software can be independently executed without interfacing with User Defined Programs (UDP). The buildings simulator is connected to the CPS through a common interface. Similarly, other UDPs can be connected to the CPS through this interface. UDPs are stand-alone software elements (subroutines); they may get some inputs from the CPS and return some outputs to the CPS. For instance, the building simulator gets surface temperatures and moisture conditions from the CPS and returns the zone air temperatures and moisture conditions to the CPS through the interface.

During each iteration or time step, certain parameters can be modified through User Defined Routines (UDR). These modifications can be local or global (see Figure 1-1). Local modifications are performed on an element level - i.e. field variable dependent material properties and/or boundary conditions. Global modifications are performed at the beginning of an iteration or time step. Examples of global modifications are time dependent material properties or boundary conditions, variable time-step simulations, numerical solution schemes (direct iteration versus Newton type iterations) etc.

1.2 Scope of Present Work

The U.S. EPA and the SRI monitored and collected data of indoor pressures and radon concentrations in a large school building at Bartow, Florida. Data under several test conditions were obtained. FSEC used the integrated computational software, FSEC 3.0, to simulate HVAC system and multizone airflows, indoor pressures, radon transport in the soil and slab and indoor radon levels in the large building. The simulation was validated by measured data. A limited parametric study shows the influence of outdoor airflow, ambient radon level and soil radium content on indoor radon levels.

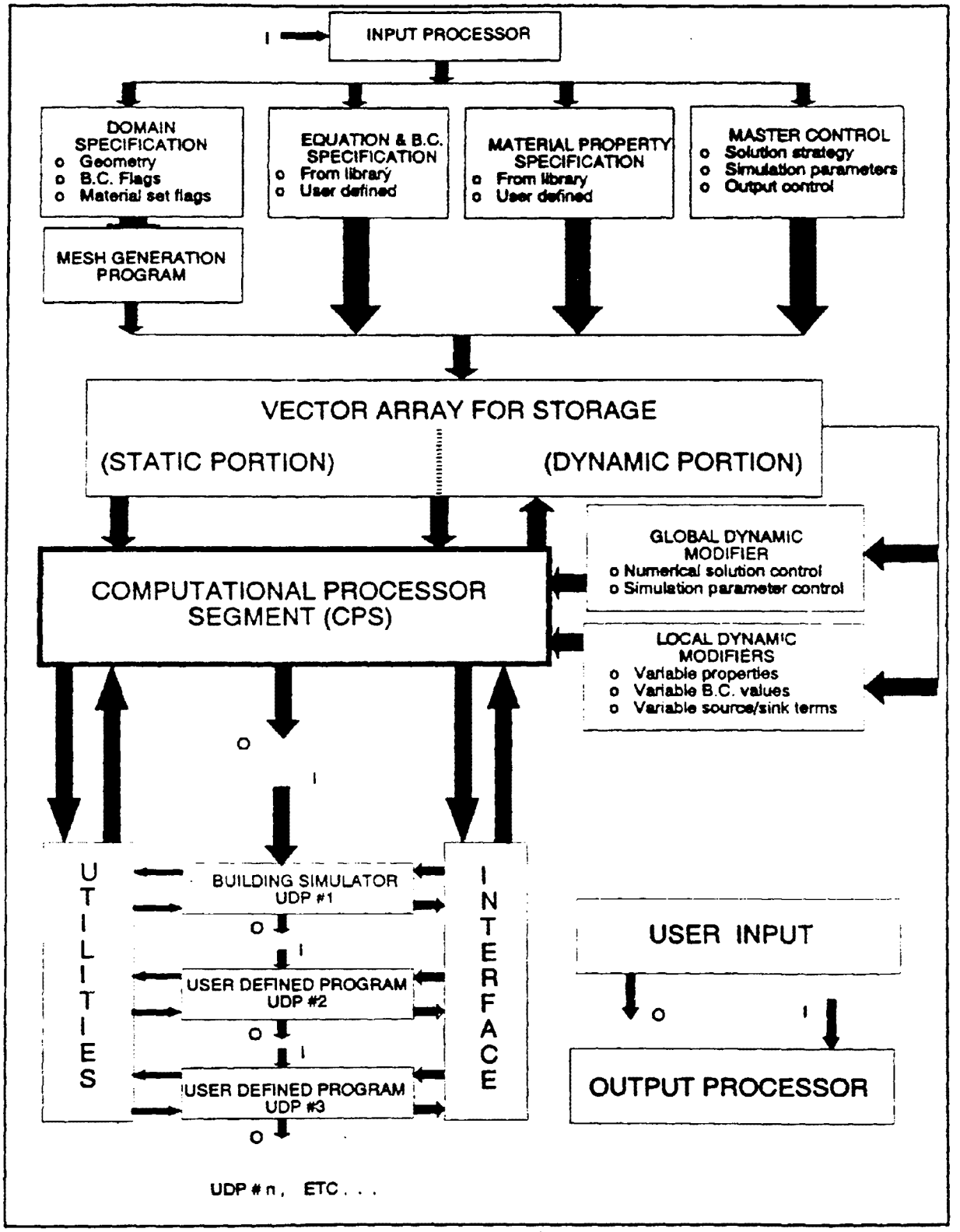

Figure 1-1. FSEC 3.0 software structure and interfaces.

2. RADON TRANSPORT AND HVAC SYSTEM

2.1 Introduction

The governing equations for radon transport and diffusion in soil and slab, radon balance, multizone airflows and zone pressures are presented in this Chapter. Pressure and radon transport equations in soil and slab were primarily obtained from information and sources provided by Rogers & Associates Engineering, Inc. (Rogers & Nielson, 1991). The air distribution system model was integrated from AIRNET, developed by the National Institute of Science and Technology (Walton, 1989). Since these mathematical formulations can be found in the references, only brief descriptions are given in this Chapter.

2.2 Radon Transport and Pressure Equation

The pressure equation, derived from Darcy's equation for flow through a porous media, is given by (Yuan & Roberts, 1981):

$$\frac{\partial P}{P_o \partial \tau} = \nabla \cdot \left(\frac{K}{\mu} \nabla P \right) \tag{2-1}$$

It should be noted that Darcy's law is valid for a Reynolds number $R_{eK} < 1$ (Cheng, 1985), where R_{eK} is Reynolds number based on air permeability and defined as $\rho v K^{1/2}/\mu$.

Radon concentration balance (Rogers & Nielson, 1991) including multiphase radon generation and transport in porous media may be expressed as:

$$\frac{\partial C_a}{\partial \tau} = \nabla \cdot D_c \nabla C_a - \frac{K_c}{\mu} \nabla P \cdot \nabla C_a - \lambda C_a + R \rho \lambda E_c \tag{2-2}$$

where

P	Pressure [Pa]
P_o	Reference pressure [Pa]
τ	Time [s]
K	Bulk air permeability in porous media [m^2]
μ	Dynamic air viscosity [1.8×10^{-5} Pa.s]
C_a	Radon concentration [Bq/m^3]
D_c	Effective radon diffusion coefficient [m^2/s]
K_c	Effective air permeability in porous media [m^2]
λ	^{222}Rn decay constant [2.1×10^{-6} s^{-1}]
R	Soil ^{226}Ra concentration [Bq/kg]
ρ	Bulk dry density [kg/m^3]

E_c Effective ^{222}Rn emanation coefficient [dimensionless]

2.3 HVAC System (Duct and multizone airflow and pressure)

Mathematical formulations of several elements of the HVAC system used in the present simulation are listed below.

Power law element - CRACKS

Based on the power law, the airflow through a cracks is expressed as

$$\dot{m}_{ij} = C_{m,j}(\Delta P)^{n_j} = C_{m,j}(P_i - P_j)^{n_j} \qquad \textbf{(2-3)}$$

where $\dot{m}$ is mass flow rate [kg/s]. $C_{m,j}$ is the flow coefficient at the j-th crack and ΔP is pressure difference across the crack. "i" indicates the i-th zone where air flow enters and "j" indicates the j-th zone or specific ambient condition where air flow leaves. "n_j" is exponent of flow equation at the j-th crack. For simplicity, it is assumed that there is one crack connected between i-th and j-th zones in the brief description. Therefore, the j-th crack is located between i-th and j-th zones. However, multiple cracks between two zones are allowable in the integrated FSEC 3.0 If it is assumed that J cracks exist in the i-th zone, the crack air flow in the i-th zone may be written as follows

$$\begin{aligned}
\dot{m}_{i,1} &= C_{m,1}(P_i - P_1)^{n_1} \\
\dot{m}_{i,2} &= C_{m,2}(P_i - P_2)^{n_2} \\
&\cdots\cdots \\
\dot{m}_{i,j} &= C_{m,j}(P_i - P_j)^{n_j} \\
&\cdots\cdots \\
\dot{m}_{i,J} &= C_{m,J}(P_i - P_K)^{n_J}
\end{aligned} \qquad \textbf{(2-4)}$$

Based on mass conservation, total mass flow should be equal to zero in the steady-state condition, that is

$$\dot{m}_i = \sum_{j=1}^{J} \dot{m}_{ij} = 0 \qquad \textbf{(2-5)}$$

By substituting the air flow of each crack in the i-th zone, Eq. (2-4) into Eq. (2-5), the air flow

of the i-th zone may be rewritten as

$$P_1)^{n_1} + C_{m,2}(P_i - P_2)^{n_2} + \ldots + C_{m,j}(P_i - P_j)^{n_j} + \ldots + C_{m,J}(P_i \quad \textbf{(2-6)}$$

In general, the expression of the i-th zone air flow may be written as

$$f_i(P_1, P_2, \ldots, P_j, \ldots, P_J) = 0 \quad \textbf{(2-7)}$$

Duct System

The pressure loss in ducts due to friction is given by

$$\Delta P_f = f \frac{L}{D} \frac{\rho v^2}{2} \quad \textbf{(2-8)}$$

where

f	Friction factor
L	Duct length
D	Hydraulic diameter
v	Velocity

The dynamic losses due to the fitting is

$$\Delta P_d = C_o \frac{\rho v^2}{2} \quad \textbf{(2-9)}$$

where

C_o	Dynamic loss coefficient

The total pressure loss in a duct is

$$\Delta P = \Delta P_f + \sum \Delta P_d \quad \textbf{(2-10)}$$

Rewriting the above equations in terms mass flow rather than velocities, one obtains

$$\dot{m} = \left(\frac{2\rho A^2}{f\frac{L}{D} + \sum C_o} \right)^{1/2} \Delta P^{1/2} \quad \textbf{(2-11)}$$

where A is the cross section area and f can be calculated by using the non-linear Colebrook

equation

$$\frac{1}{f^{1/2}} = 1.44 - 2.0\ln\left(\frac{D}{\epsilon}\right) - 2.0\ln\left(1+\frac{9.3}{Re\frac{\epsilon}{D}f^{1/2}}\right) \qquad \textbf{(2-12)}$$

and where

ϵ Surface roughness

Re Reynolds number

Reynolds number is defined as

$$Re = \frac{\rho VD}{\mu} = \frac{\dot{m}D}{A\mu} \qquad \textbf{(2-13)}$$

Fan Element

Fan performance is normally characterized by a performance curve, which relates the total pressure rise to the flow rate for a given fan speed and air density. The performance curve may be represented by cubic polynomials:

$$\Delta P = a_o + a_1\dot{m} + a_2\dot{m}^2 + a_3\dot{m}^3 \qquad \textbf{(2-14)}$$

where

ΔP fan total pressure rise = the fan total pressure at outlet minus the fan total pressure at inlet [Pa]

$a_0 \ldots a_3$ Coefficients of the polynomial

The performance of a given fan at various speed and air densities may be related to a single fan performance curve through the "FAN LAW"

$$\frac{Q_1}{Q_2} = \left(\frac{N_1\rho_1}{N_2\rho_2}\right) \qquad \textbf{(2-15)}$$

and

$$\frac{\Delta P_1}{\Delta P_2} = \left(\frac{N_1^2\rho_1}{N_2^2\rho_2}\right) \qquad \textbf{(2-16)}$$

where

Q	Volume flow rate [m^3/s]
N	Fan rotational speed

2.4 Zone Radon Balance Equations

The indoor radon balance equation at the i-th zone may be written as follows

$$V_i \frac{\partial C_{a,i}}{\partial \tau} - F_{entry,i} + Q_{inf,i}(C_{a,\infty} - C_{a,i}) + \sum_{j=1}^{noz} Q_{j-i}(C_{a,j} - C_{a,i}) \qquad \textbf{(2-17)}$$

where

i	i-th zone
j	j-th zone
V	Zone volume [m^3]
C_a	Indoor radon concentration [Bq/m^3]
$C_{a,\infty}$	Ambient radon concentration [Bq/m^3]
F_{entry}	Radon entry from the slab [Bq/s]
Q_{j-i}	Indoor air flow from j-th zone to i-th zone [m^3/s] ($Q_{i-i}=0$)
Q_{inf}	Infiltration from ambient [m^3/s]
noz	Number of zones

It should be noted that Q_{inf} is considered return flow to the building return plenum in the present simulation. The ambient radon concentration will be modified by combining all return flows from all zones with the outdoor air flow. Its expression is

$$C_{a,\infty} = \frac{Q_{OA}C_{\infty} + \sum Q_{inf,i}C_{a,i}}{Q_{OA} + \sum Q_{inf,i}} \qquad \textbf{(2-18)}$$

where

Q_{OA}	Outdoor airflow rate through the air distribution system [m^3/s]
C_{∞}	Ambient radon concentration [Bq/m^3]

3 PRELIMINARY SIMULATION

3.1 Introduction

Before detailed simulation of indoor radon concentration and radon entry from the slab, the air distribution system should be simulated to calculate indoor pressures and multizone airflows. Based on the design data from the air conditioning plan by the Langbein & Bell Engineers and testing data from the testing and balancing report by the Associated Air Balance Council, the input file for the HVAC system simulation was created. By refining parameters of each component, acceptable results were obtained and compared with design and testing data. Indoor pressures, multizone airflow rates and terminal flow rates through the duct system were calculated in the HVAC system simulation.

3.2 Simulation Procedure

The efforts for the preliminary simulation are described below.

List and characterize all components of HVAC system

Based on the air conditioning plan of the building, the HVAC system has to be discretized into a number of component elements used in the simulation. Components are composed of ducts with different cross section and lengths, VAV boxes, fans, etc. Individual VAV box or the fan is considered to be one element, and ducts with the same shape and cross section are also considered to be one element. The parameters of most elements required for the simulation were obtained from the ASHRAE handbook, the US EPA publications, or other sources. However, where the parameters of some elements are not known, a best guess was assigned for initialization and these parameters were adjusted in comparison to experimental data.

Input file preparation

When discretization of the HVAC system and characterization of each element are accomplished, the input file, which consists of the node number, element number, element type for different components, and nodal connectivity of each element, is created.

Simulation and refinement

By trial and error, adjustment of some parameters with the initialized best guess are made through test simulations. All the parameters used in the HVAC system are calibrated through refinement process to match measured data.

3.3 Preliminary Simulation Results

The preliminary simulation results show the terminal airflow rate comparison between the design and simulation, and testing data and simulation, respectively. Constant inlet flow from the fan

is assigned and indoor air pressures are set to zero gauge. The VAV boxes are assumed to be fully open. Figure 3-1 shows the schematic of the air conditioning plan of the building with terminal nodal numbers.

Table 3-1 shows the comparison of design and simulation air flow rates based on the air conditioning design plan. The purpose is to create an input file with duct component parameters needed in the simulation for further refinement of component parameters. The first column indicates the node number, corresponding to each terminal listed in Figure 3-1. The second and third columns show that airflow rates at each terminal, corresponding to the node number in the first column, from design and simulation, respectively. The fourth column lists the percent difference. A maximum 6.04% difference, as shown in the Table 3-1, was observed between prediction and design data. It should be noted that some design deficiencies were found and will be discussed later. The last row in Table 3-1 is total inlet air flow rates of design and simulation.

Table 3-2 shows the comparison of measured and predicted airflow rates at each terminal, based on the Testing and Balancing Report. The Report presents real performance of the HVAC system for different VAV boxes and terminals. Due to the difference of HVAC system performance between testing and design, some component parameters are adjusted compared with the first simulation. The second and third columns list the measured and predicted airflow rates, respectively, corresponding to nodal number in the first column. The fourth column shows the percent relative difference. A maximum difference of 4.62% was obtained. The last row in Table 3-2 is total measured and predicted inlet airflow rates.

It should be pointed out that discrepancy exists between design and testing. For example, maximum outdoor airflow rate is 1200 cfm, according to the air conditioning design plan. However, results from a recent testing and balancing report showed the maximum outdoor airflow of 3047 cfm. The performance of some VAV boxes from testing report differs from design. Therefore, corresponding adjustments are necessary. Since the testing data show the present HVAC system performance, parameters adjusted by comparison to testing data are used in subsequent simulation.

3.4 Closure

Excellent comparison between testing or design and predicted airflow rates have been obtained. Airflow validation is based on the current parameters of duct, fan and cracks. Multizone airflows and indoor pressures will be used in calculation of radon entry through the slab and indoor radon level.

Some changes, compared to design, of the building HVAC system are found. For example, main duct size, connected to terminals defined in Nodes 57, 59, 62, 64, 67, 69, 72 and 74 in the Cafeteria, were changed from 20" diameter to 15" diameter, (Figure 3-1), so that it is hard to achieve 500 CFM for each terminal, if the duct size connected to these terminals are the same. FSEC 3.0 can air in the design or redesign of the HVAC system.

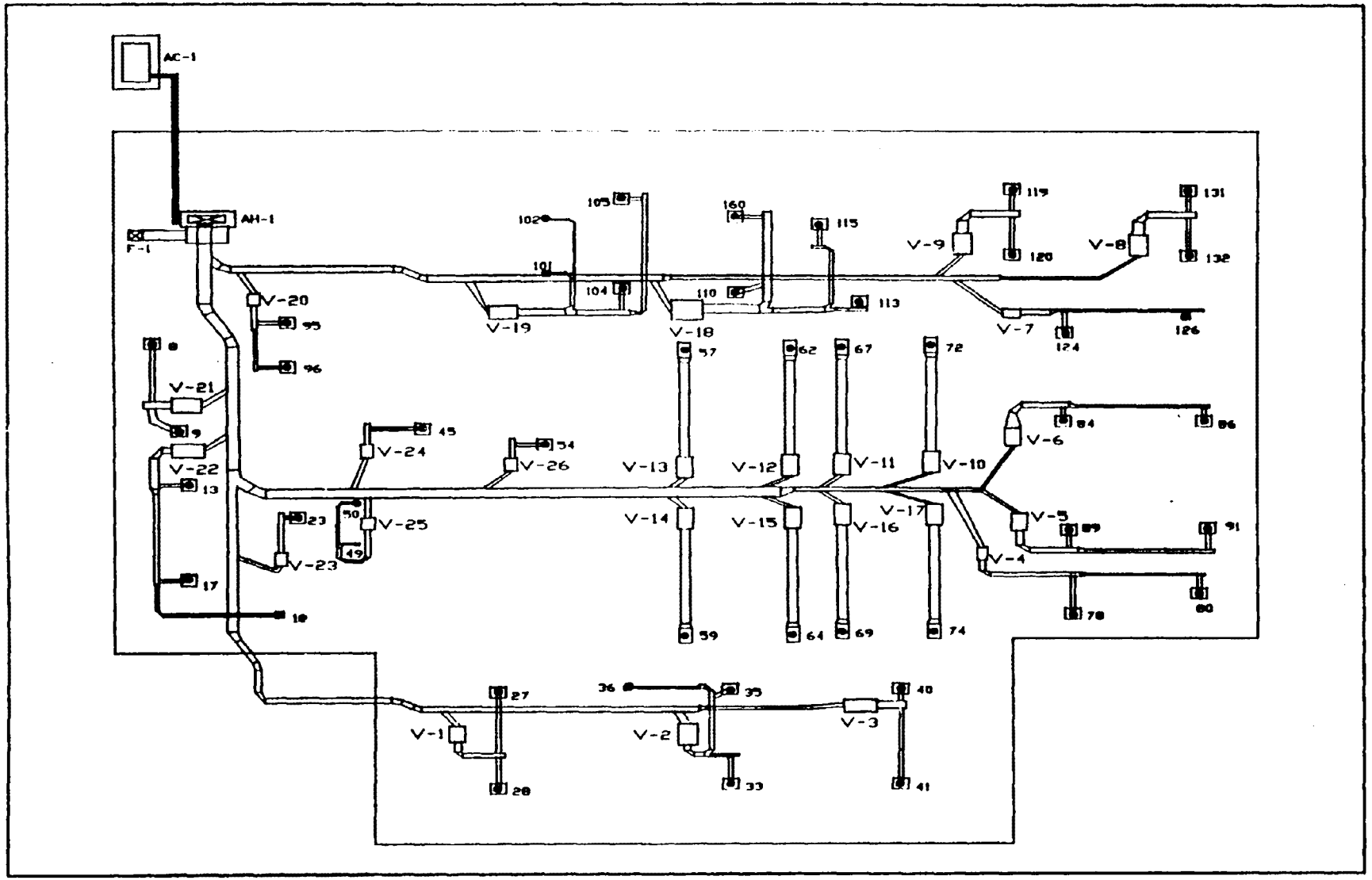

Figure 3-1. Schematic of air conditioning plan at Polk Life and Learning Center.

Table 3-1. Comparison of airflow rate between design and simulation

Node No.	Design cfm	Simu. cfm	% diff.
8	175	173	-1.13
9	365	359	-1.38
13	140	139	-0.25
15	150	150	0.44
17	175	174	-0.40
18	275	276	0.42
23	115	115	0.07
27	200	202	1.46
28	230	236	2.61
33	230	228	-0.46
35	220	218	-0.47
36	70	70	0.08
40	225	220	-1.88
41	260	255	-1.80
45	130	132	1.84
49	75	77	3.56
50	50	51	2.68
54	120	123	2.72
57	500	509	1.87
59	500	509	1.87
62	500	500	0.12
64	500	500	0.12
67	500	520	4.20
69	500	520	4.20
72	500	510	2.06

(continued)

Table 3-1 (continued)

Node No.	Design cfm	Simu. cfm	% diff.
74	500	510	2.06
78	145	148	2.62
80	85	86	2.14
84	210	209	-0.47
86	240	245	2.36
89	210	207	-1.39
91	240	230	-3.77
95	70	71	2.61
96	75	76	2.17
101	165	174	5.75
102	100	96	-3.01
104	100	93	-6.04
105	250	262	5.13
110	325	309	-4.69
113	325	315	-3.02
115	325	315	-3.05
119	210	210	0.34
120	200	199	-0.07
124	100	98	-1.06
126	50	48	-3.07
131	250	236	-5.44
132	250	242	-2.90
160	325	315	-2.96
Total	11455	11460	0.044

Table 3-2. Comparison of airflow rate between measurement and simulation at testing condition

Node No.	Meas cfm	Simu cfm	% diff
8	80	81	1.87
9	175	178	1.93
13	150	151	0.73
17	130	131	1.35
18	220	223	1.44
23	105	107	1.91
27	125	127	2.23
28	130	133	2.40
33	140	143	2.31
35	95	97	2.31
36	35	35	2.55
40	165	162	-1.57
41	180	177	-1.57
45	120	120	0.64
49	65	65	0.46
50	40	40	0.69
54	100	97	-2.14
57	320	314	-1.67
59	320	314	-1.67
62	500	484	-3.12
64	490	484	-1.14
67	460	453	-1.45
69	480	471	-1.82
72	490	487	-0.56
74	510	502	-1.47

(continued)

Table 3-2 (continued)

Node No.	Meas cfm	Simu cfm	% diff
78	80	80	0.80
80	60	60	1.35
84	140	143	2.19
86	140	143	2.49
89	135	138	2.63
91	135	138	2.59
95	50	51	2.39
96	50	51	2.50
101	100	99	-0.59
102	55	54	-0.40
104	55	55	1.53
105	150	151	1.12
110	225	229	2.16
113	225	233	3.93
115	225	233	3.79
119	150	156	4.14
120	140	143	2.76
124	110	114	3.73
126	50	52	4.62
131	145	144	-0.21
132	150	148	-1.00
160	225	233	3.96
Total	8421	8424	0.036

4 VALIDATION

4.1 Introduction

Following the preliminary simulation of airflow in the HVAC system of Polk Life and Learning Center in Bartow, Florida, multizone airflows, zone pressures, indoor radon concentrations, and radon entry rates from the slab were simulated and compared with experimental data during certain time periods, using the integrated FSEC 3.0 software. This Chapter describes the comparison. It should be noted that calibration of parameters in the last Chapter is for the HVAC system only. The parameter calibration in this Chapter relates to radon transport in the soil and slab. After calibration, the simulation is compared to measured data for one typical school day.

4.2 Geometry Description of Soil and Concrete Slab

Soil and Slab

In order to correctly model radon entry, a 3-D soil and slab discretization becomes necessary to obtain radon entry and indoor radon levels for different indoor pressures at different zones. The schematic of 3-D mesh is shown in Figure 4-1. It should be noted that the large elements are used in the present simulation to reduce computational time. Since cracks are not discretized separately, weighted-average properties of air and concrete are used for the element. These properties will be adjusted based on the crack size at each element.

Zone

According to the experimental layout and observation from Polk Life and Learning Center, seven (7) zones are used in the present simulation, as shown in Figure 4-2. These zones are labeled Room 102 for Zone 1, Conference room for Zone 2, Cafeteria for Zone 3, Rm 105 for Zone 4, Audiology Room for Zone 5, Room 109 for Zone 6 and Corner room for Zone 7, respectively. It should be noted that measurement data are available in Zones 1, 2, 3, 5 and 6.

4.3 Simulation Results Compared to Full Airflow

A special experiment is set up in order to control VAV box performance and establish the calibration for VAV boxes. Thermostats in all zones are set to 6°F lower than the normal setting, and fan airflow is set to the maximum, so that VAV boxes in the duct system can be assumed to be fully open. Since the VAV box is controlled by temperature differences between zones and thermostats, the special setting was required to avoid adjusting parameters related to VAV box performance in the simulation. Time period for the experiment was from 12:30 PM to 7:00 PM on April 4, 1993. Figures 4-3 to 4-7 shows comparisons of simulations to measurements during this time period for the Cafeteria, Room 109, Room 102, the Audiology Room and the Conference Room, respectively. From the observation of measured data, mentioned by Marc Menetrez (EPA), and suggested by Bobby Pyle (SRI), the lowest

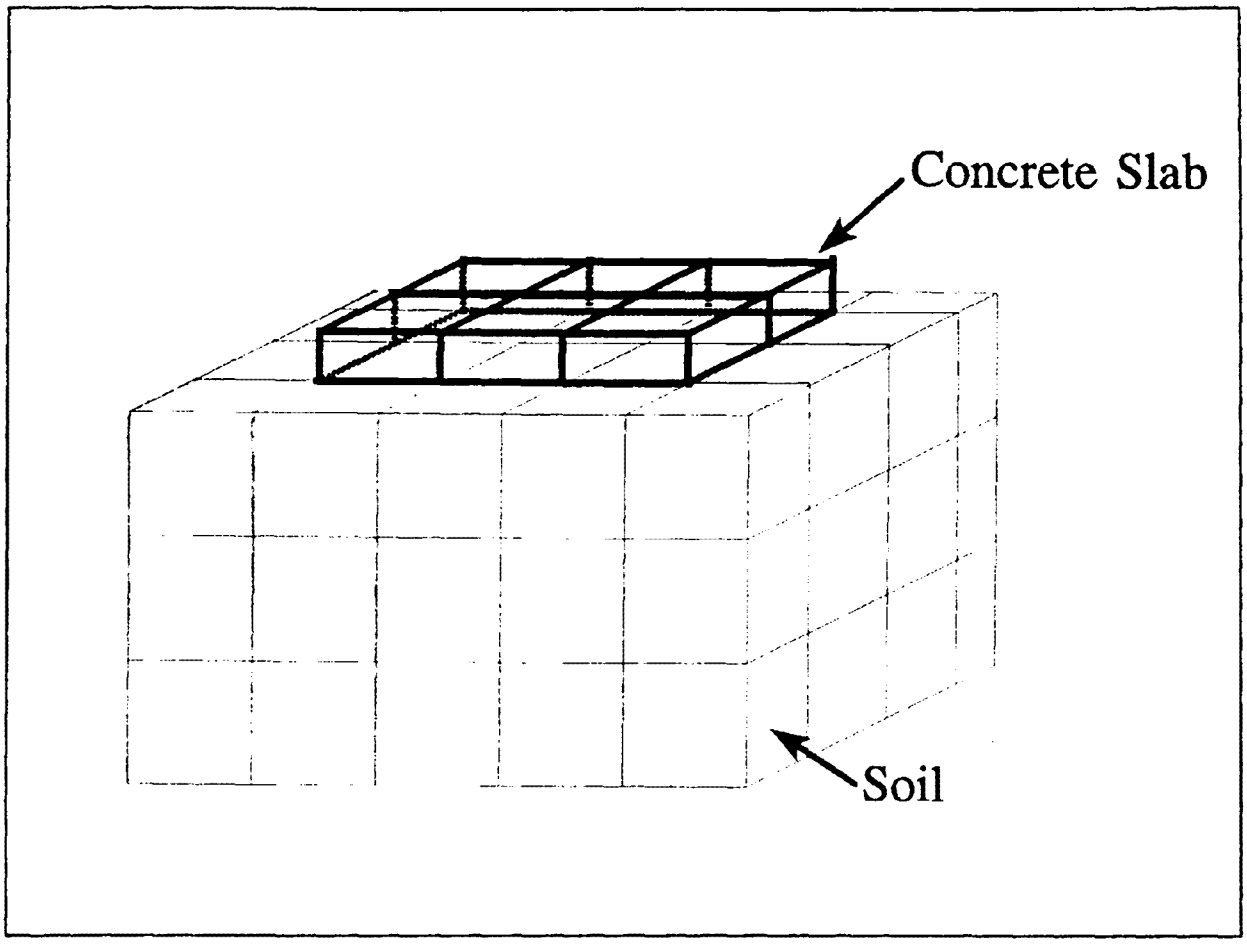

Figure 4-1. Schematic of three dimension mesh configuration.

indoor radon concentration are comparable to the ambient radon level. In this case, outdoor radon concentration is set to 5 pCi/L. Further, during this validation, the radon entry rate can be calculated based on precalculated indoor pressures obtained by computing airflow rates through the air conditioning system. Two steps of the building simulation, steady-state and transient conditions, are used to refine the material properties of soil and concrete slab used in the input file.

Validation at Steady-State Condition

The purpose of steady-state simulation is to adjust material properties of soil and slab, such as diffusion coefficient, emanation coefficient, air permeability, moisture content, etc. In other words, radon entry rate from the slab will be calibrated, comparing simulated indoor radon level with experimental data. As mentioned before, some material properties of the concrete slab, especially for radon diffusion coefficient and air permeability, represent the properties of combined concrete and crack by estimating crack size for each element of the slab. Therefore, as long as a reasonable comparison is obtained, the material property estimation is considered

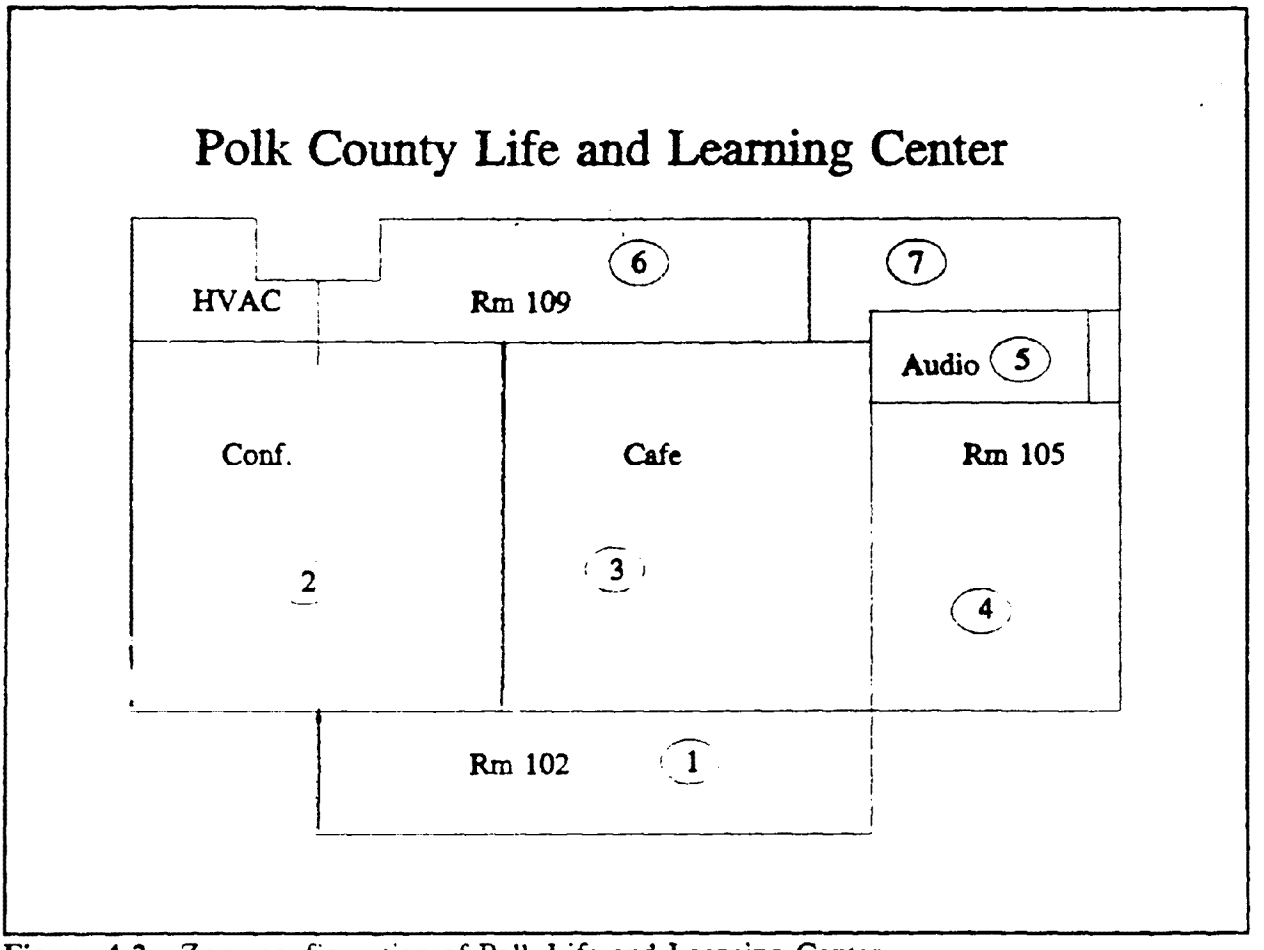

Figure 4-2. Zone configuration of Polk Life and Learning Center.

reasonable. The radon concentration and pressure distribution in the soil and slab will be used as the initial conditions for transient simulation during the seven (7) hour time period. It should be noted that the measured data of fan and outdoor airflows at 7:00 PM are used as steady-state inputs. It was observed from experimental data that fan and outdoor airflows change very little during the seven-hour period, so that these flows are essentially constant.

Table 4-1 lists all airflows from the present simulation for the air distribution system. The first column gives nodal connectivity for each element used in the simulation. These elements represent those from terminals to zones, zone to zone, and zone to return plenum. Nodal connectivity shows element connection between two nodes, where the first node indicates the air inlet and the second the air exit. In the simple terminology, inlet node is called "from" and exit node is called "to". The negative sign indicates the airflow direction is opposite to the direction of nodal connectivity. The other three columns are airflow rates, expressed in different units. It is assumed that air density is 1.2 kg/m^3.

Table 4-1. Multizone and terminal airflow rate from simulation of air distribution system

Nodal Connectivity	Airflow Rate (kg/s)	Volume Flow Rate (cfm)	Volume Flow Rate (m^3/s)
173-179	-0.1871	-336	-0.1586
174-179	-0.2021	-364	-0.1717
175-179	-0.3299	-592	-0.2795
176-179	-0.0141	-25	-0.0119
177-179	-0.2712	-487	-0.2298
178-179	-0.0543	-98	-0.0460
173-180	0.7996	1,436	0.6776
174-180	0.7949	1,427	0.6736
175-180	0.7432	1,334	0.6298
176-180	0.0725	130	0.0614
177-180	0.7699	1,382	0.6525
178-180	0.7960	1,429	0.6746
179-180	0.8304	1,491	0.7037
173-178	0.0543	98	0.0460
173-174	0.0631	113	0.0535
177-178	-0.1668	-300	-0.1414

Table 4-2 lists the gauge pressures (relative to ambient) at different zones obtained from simulation and measurement. RAP and Amb indicate the return air plenum and ambient, respectively. All pressures are relative to the ambient pressure. Very good agreement between prediction and measurement has been achieved. In other words, the simulation results correctly reflect the HVAC system performance in the building. When the air handing unit is on, the zones are pressurized, as shown in Table 4-2. Evidently, advection of radon through cracks carried by air flow may be negligible with positive pressure in the building. The diffusion of radon through the slab is the main factor that affects indoor radon level compared to advection.

Table 4-2. Comparison of indoor pressures between simulation and measurement

Node Number	Relativity	Measured (Pa)	Simulated (Pa)
180	RAP-Amb.	1.50	1.50
172	Cafe.-Amb.	2.11	2.11
171	Rm 109-Amb.	2.19	2.19
169	Audio.-Amb.	1.95	1.81
167	Rm 102-Amb.	1.68	2.12
166	Conf.-Amb.	2.12	2.12

Table 4-3 shows good agreement between simulated and measured values of indoor radon levels. Although seven zones are used in the simulation, results of simulation show only indoor radon concentrations in five zones, because only five zones are measured in the experiment.

Table 4-3. Comparison of indoor radon levels between simulation and measurement

Zone Number	Measured (pCi/L)	Simulated (pCi/L)
Cafe	5.8	6.10
Rm. 109	5.4	5.33
Audio	6.9	6.65
Rm. 102	6.3	6.26
Conf.	5.3	5.37

Validation at Transient Condition

During the validation period, the transient simulation is from 12:30 PM to 7:00 PM on 4/4/93. It should be noted that indoor pressures, fan flow, and outdoor air airflows are assumed to be constant during the validation time period. These values are the same as those at the steady-state condition. The simulation results of radon and pressure distribution in the soil and slab at the steady-state condition are used as initial conditions in the transient simulation. From Table 4-4, the radon entry rate from the slab into different zones remain fairly constant, even though indoor radon levels vary due to outdoor air dilution. In other words, radon entry rate from the slab is affected only slightly by the indoor radon level. It should be noted that radon entry rate in the individual zone is equal to radon flux multiplied by the individual zone area.

Table 4-4. Radon entry rate from different zones [Bq/s]

Time	Zone 1	Zone 2	Zone 3	Zone 4	Zone 5	Zone 6	Zone 7
13.0	41.1394	31.8613	52.2105	24.3544	0.4623	35.3662	12.6480
13.5	41.3059	31.9482	52.3159	24.3976	0.4627	35.4351	12.6701
14.0	41.3919	31.9948	52.3778	24.4254	0.4630	35.4761	12.6817
14.5	41.4320	32.0189	52.4119	24.4436	0.4631	35.4996	12.6878
15.0	41.4472	32.0305	52.4292	24.4554	0.4632	35.5124	12.6909
15.5	41.4495	32.0351	52.4366	24.4631	0.4632	35.5186	12.6923
16.0	41.4456	32.0359	52.4381	24.4678	0.4632	35.5210	12.6926
16.5	41.4398	32.0350	52.4372	24.4708	0.4633	35.5212	12.6926
17.0	41.4336	32.0333	52.4348	24.4725	0.4633	35.5204	12.6922
17.5	41.4278	32.0312	52.4319	24.4734	0.4632	35.5189	12.6918
18.0	41.4226	32.0291	52.4286	24.4735	0.4632	35.5172	12.6912
18.5	41.4187	32.0272	52.4259	24.4734	0.4632	35.5156	12.6908
19.0	41.4155	32.0255	52.4235	24.4731	0.4632	35.5140	12.6904

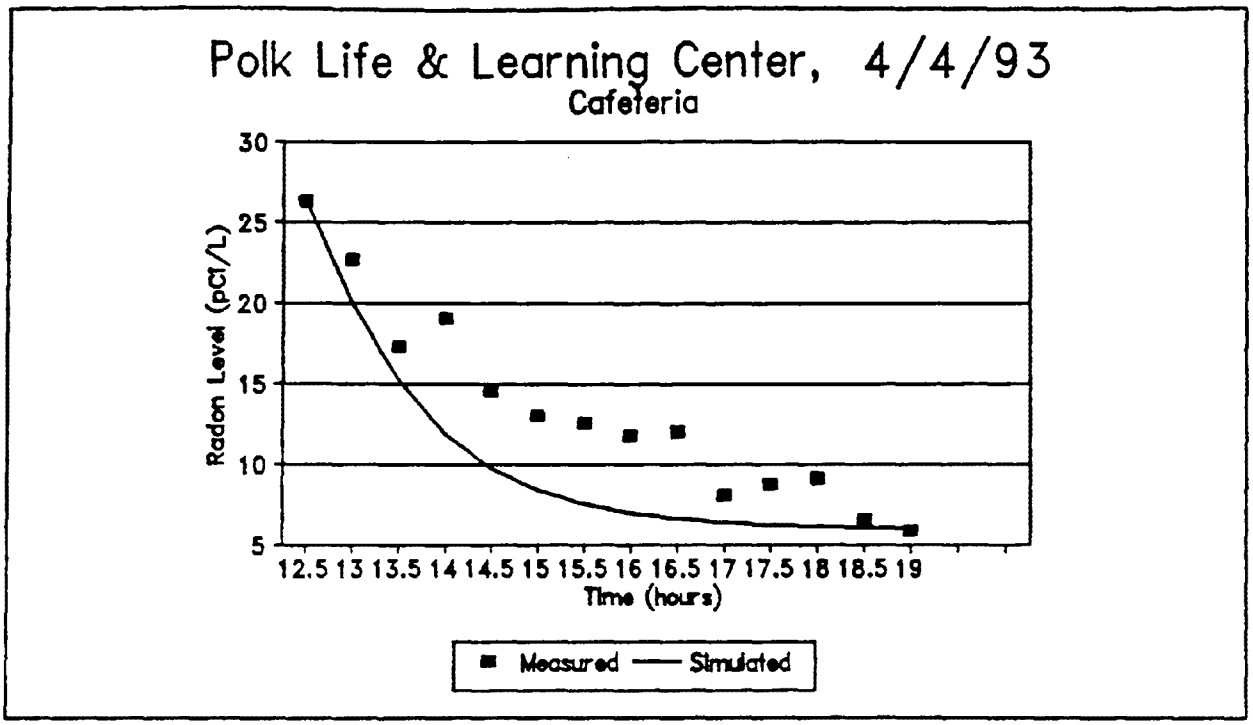

Figure 4-3. Indoor radon level comparison at Cafeteria.

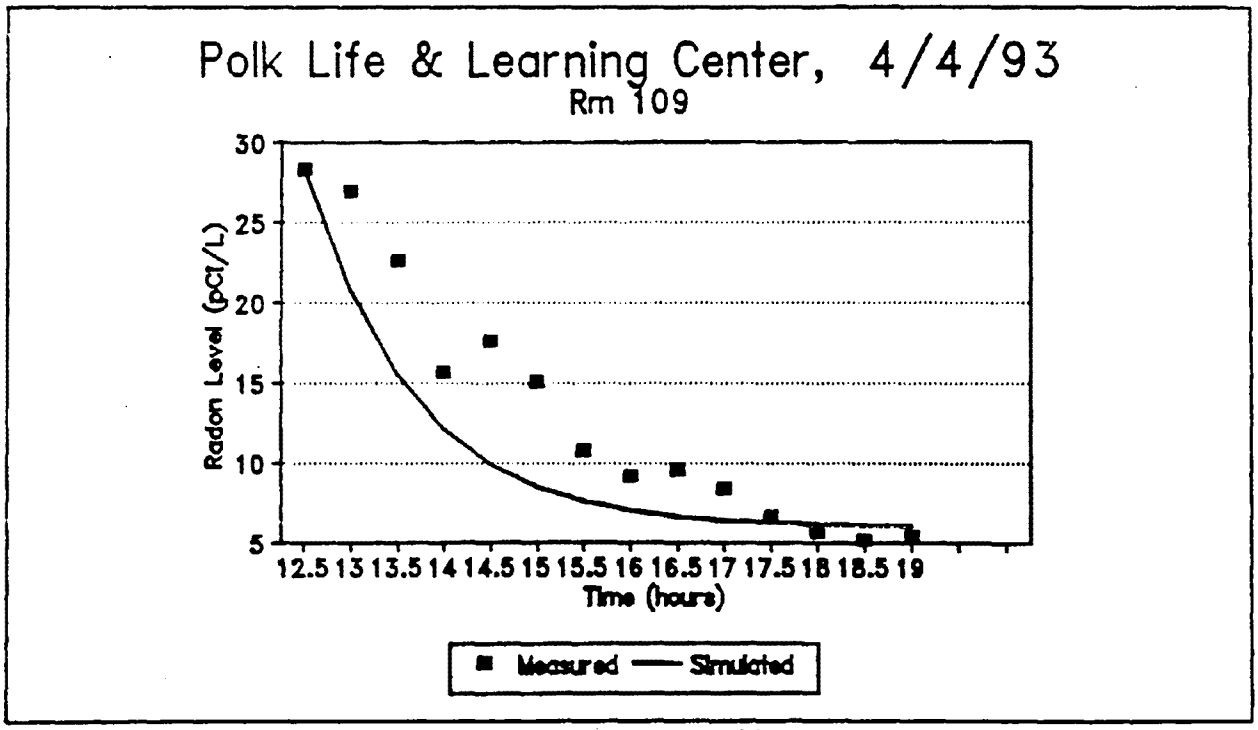

Figure 4-4. Indoor radon level comparison at Room 109.

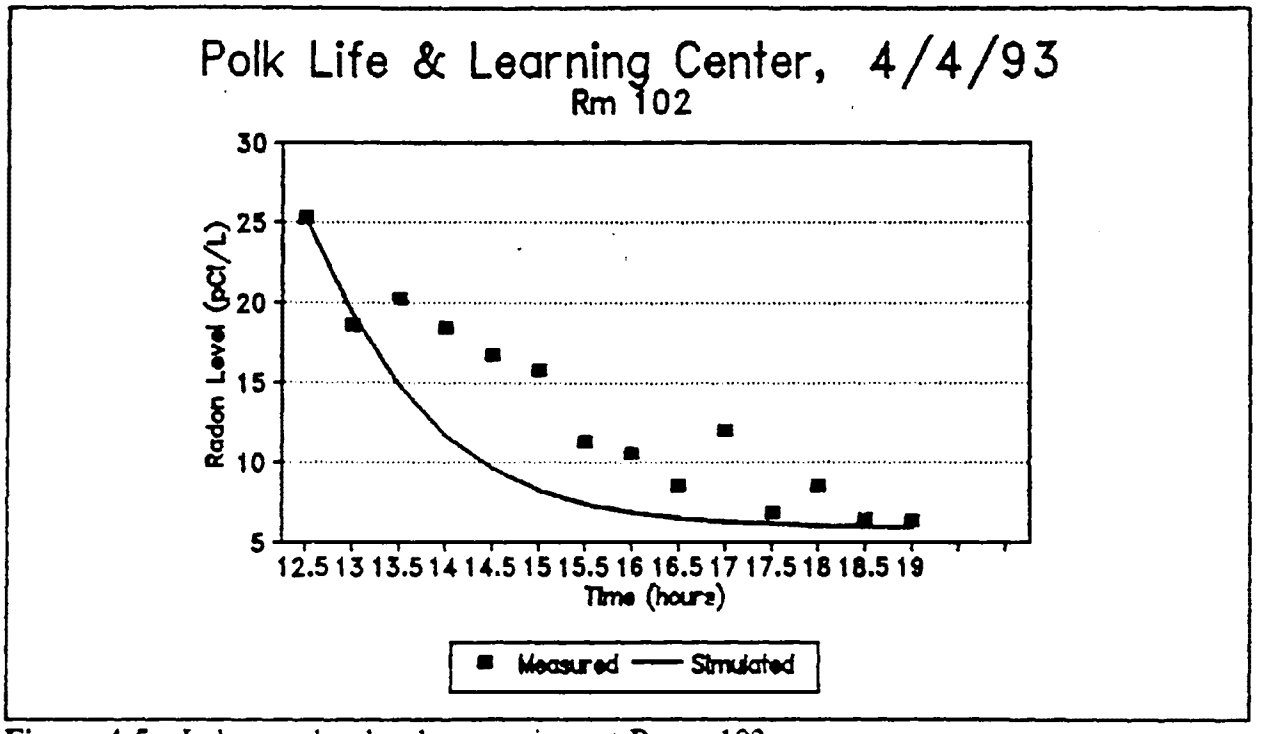

Figure 4-5. Indoor radon level comparison at Room 102.

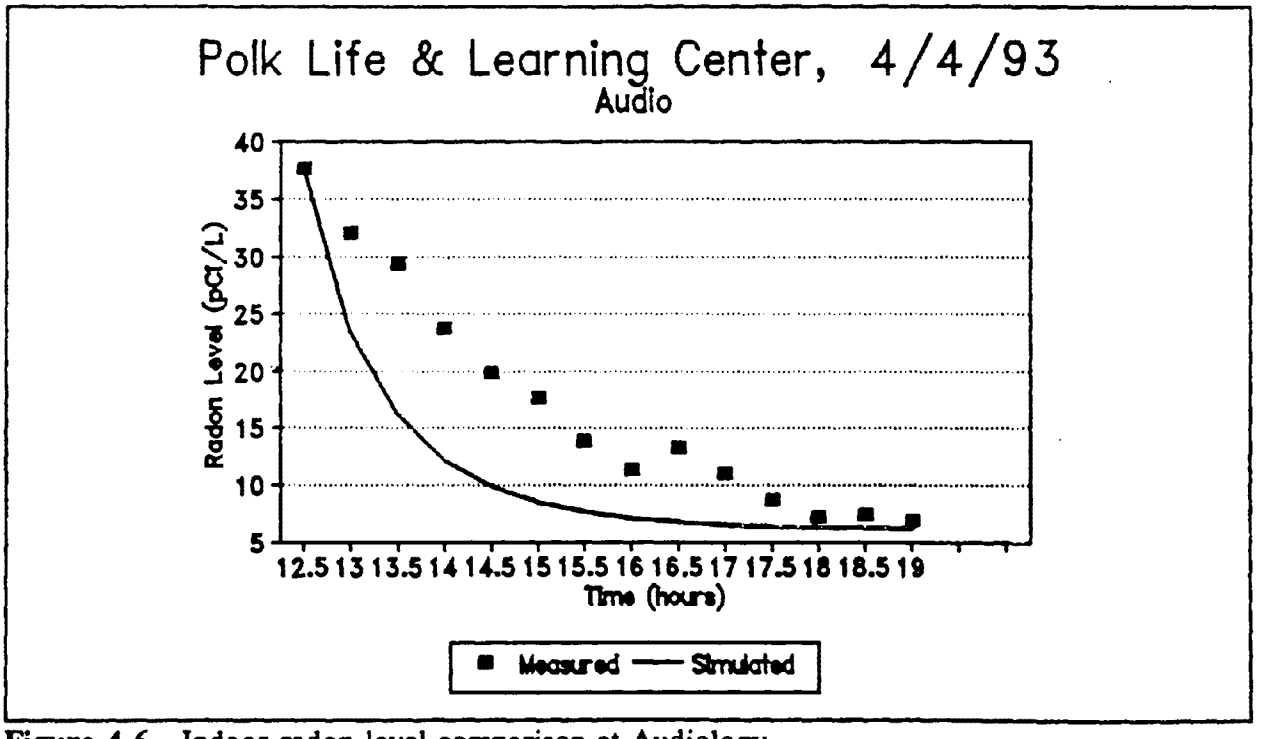

Figure 4-6. Indoor radon level comparison at Audiology.

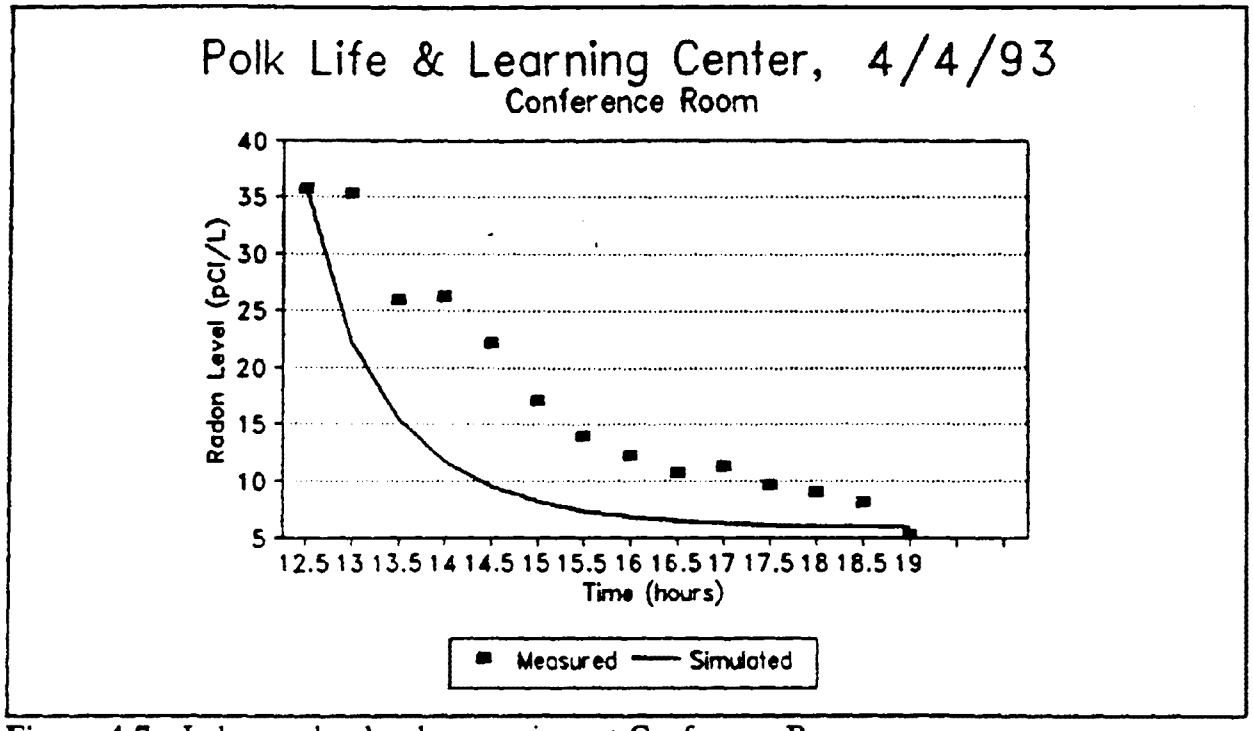

Figure 4-7. Indoor radon level comparison at Conference Room.

Figures 4-3 to 4-7 show comparisons of indoor radon levels between simulation and measurement for five (5) zones. Measured indoor radon concentrations at 12:30 PM are used as initial conditions. The airflow rates and indoor pressures remain the same as those at the steady-state condition. In order to be consistent in all simulations, the material properties in the soil and slab are kept the same. All the pressure and radon concentration distributions at the steady-state condition are also used as initial conditions for the pressure and radon transport equations. Simulation results show that dilution rate of indoor radon level due to outdoor air is faster than the measured results, although the indoor radon levels at the final hour are closer to the measured data. The explanation, first of all, is that the lumped zone air model is used in the simulation assuming 100% mixing. In reality, ventilation effectiveness is not 100%, so that indoor radon levels do not decrease as fast as indicated by the simulation. Since ventilation efficiency directly affects the simulated results, investigation of ventilation efficiency is necessary for further refinement. A correction factor for ventilation efficiency should be included in the simulation. However, these factors will be a function of flow rate, register location, zone size, etc. Detailed fluid dynamics simulation can be used to determine these factors. Secondly, the ambient radon level may be higher than assumed. Due to the unavailability of data on ambient radon levels, a constant ambient radon concentration was assumed. Finally, another more likely reason, suggested by R. Mosley (US EPA), is that the passive radon monitor being used has a slow response time and can not follow the rapid rates of change that occur.

This validation is used to calibrate radon entry rate from the slab by adjusting the material

properties of combined crack and concrete. Once the material properties are refined, they will not be changed for subsequent simulation.

4.4 Simulation Results in a Typical School Day

Following previous validation for short time periods to calibrate radon entry rate through the slab, a typical day is chosen to continue to validate simulation results of the building under study. The typical day is a normal school day starting from 6:00 AM, 4/21/93 (Wednesday) to 6:00 AM, 4/22/93 (Thursday), as suggested by Bobby Pyle, SRI. The A/C was on in the first twelve (12) hours and off in the next twelve (12) hours. When the A/C is on, certain amount of outdoor air is brought through duct system to dilute the indoor radon concentration. When the A/C is off, no outdoor air enters the zone, and indoor radon concentration increases due to radon entry from the slab. The indoor radon level increases linearly with time, based on the magnitude of radon entry rate from the slab. Figures 4-8 to 4-11 show comparisons of simulation results to measured data. The indoor radon concentration decreases during A/C on-time period and increases linearly when the A/C was off, as expected. It should be noted that since the ventilation efficiency factor is not included in the present simulation, the indoor radon level decreases faster than measured data. From observation of measurement and suggestion from SRI, ambient radon level is set to 3.5, pCi/L when A/C was on, because the minimum indoor radon level is 3.6 pCi/L. It is assumed that when A/C is on for a long time, it brings enough outdoor air throughout the building to reach the minimum indoor radon level, which is equivalent to that of the ambient condition.

4.5 Closure

It can be seen that from the figures that reasonable comparisons between prediction and measurement has been obtained. Material properties were not changed between the seven-hour calibration and the one day validation, showing the material properties used in the input file are a good approximation after adjustment. Radon entry from the slab varies slightly but may be considered to be constant during A/C on and off period. From the observation of experimental data, pressure differences between on and off periods is approximately within 1 Pa. However, there are some unknown effects causing discrepancy with measured data. The possible explanation may involve ventilation efficiency, leakage area, or possibly instrument response times. It should be pointed out that indoor positive pressures in the building are measured when A/C was on, so that advection term of radon entry from the slab is relatively small compared to indoor negative pressures. Since ambient radon level was unavailable during this period, a constant ambient radon level was assumed. Results of other work for the FRRP (see Tyson et al., 1993) show that ambient radon levels may not only be higher than established action levels, but may also vary cyclically during a 24-hour day. Clearly, the model would predict lower rates of dilution and would approach measured values if higher ambient radon levels are used in the simulation. Undoubtedly, these two factors namely, ventilation efficiency and ambient radon levels, must be investigated further before answering the question definitively.

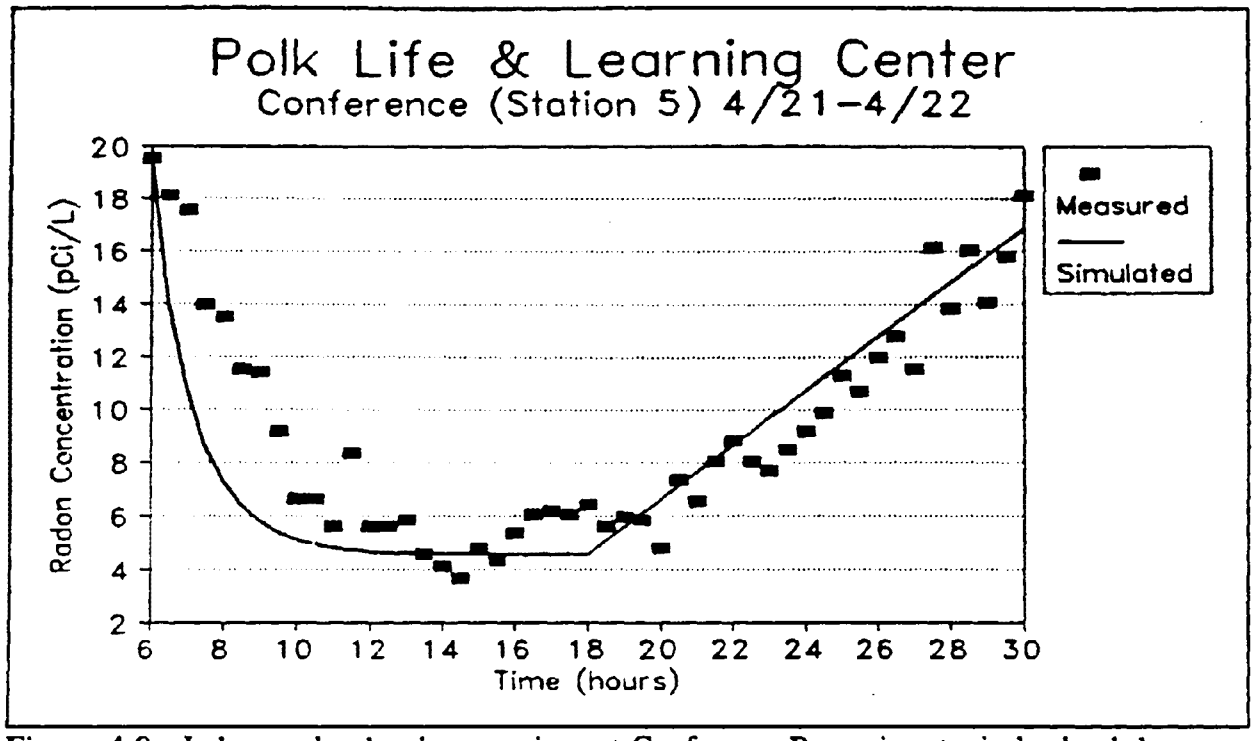

Figure 4-8. Indoor radon level comparison at Conference Room in a typical school day.

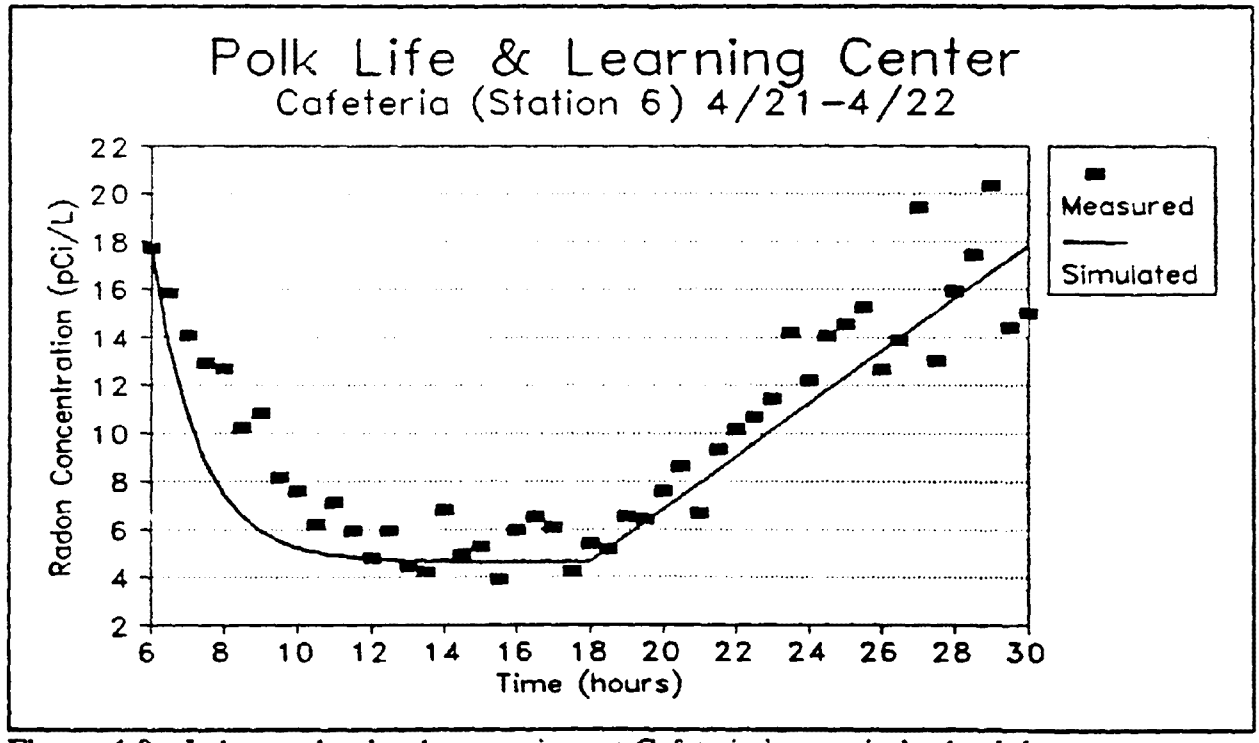

Figure 4-9. Indoor radon level comparison at Cafeteria in a typical school day.

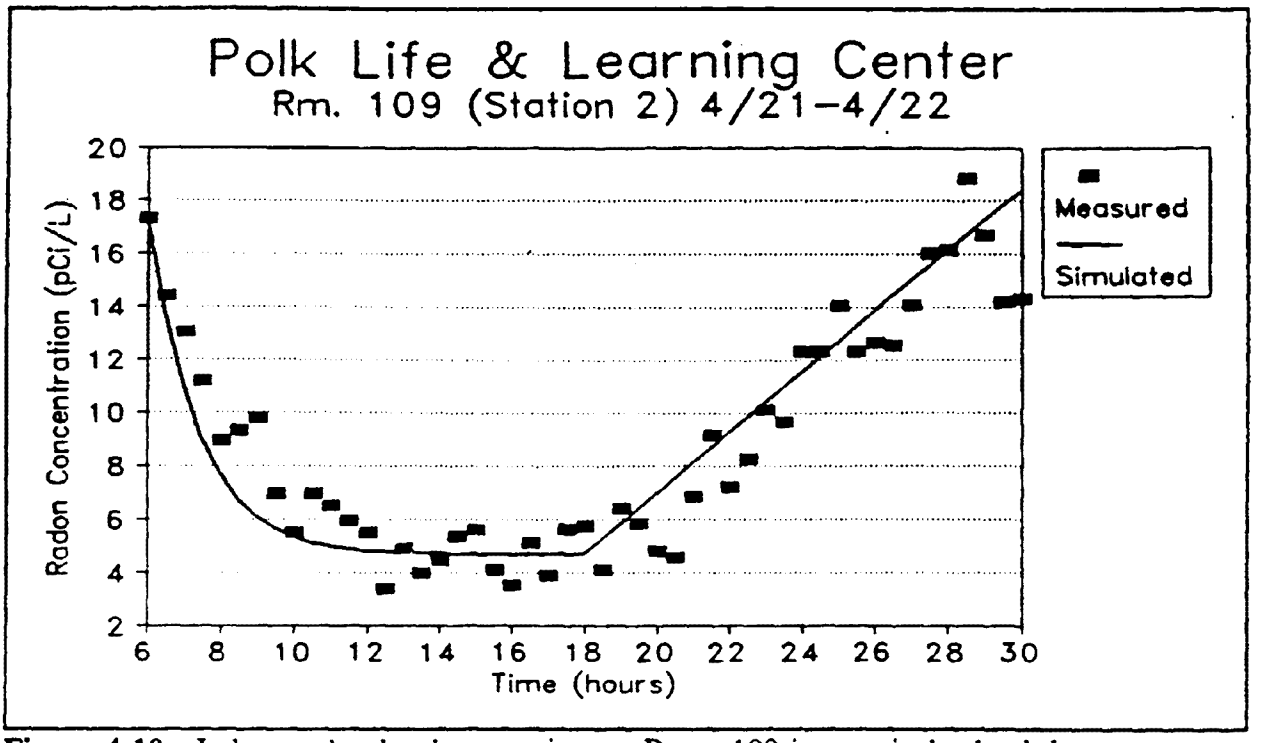

Figure 4-10. Indoor radon level comparison at Room 109 in a typical school day.

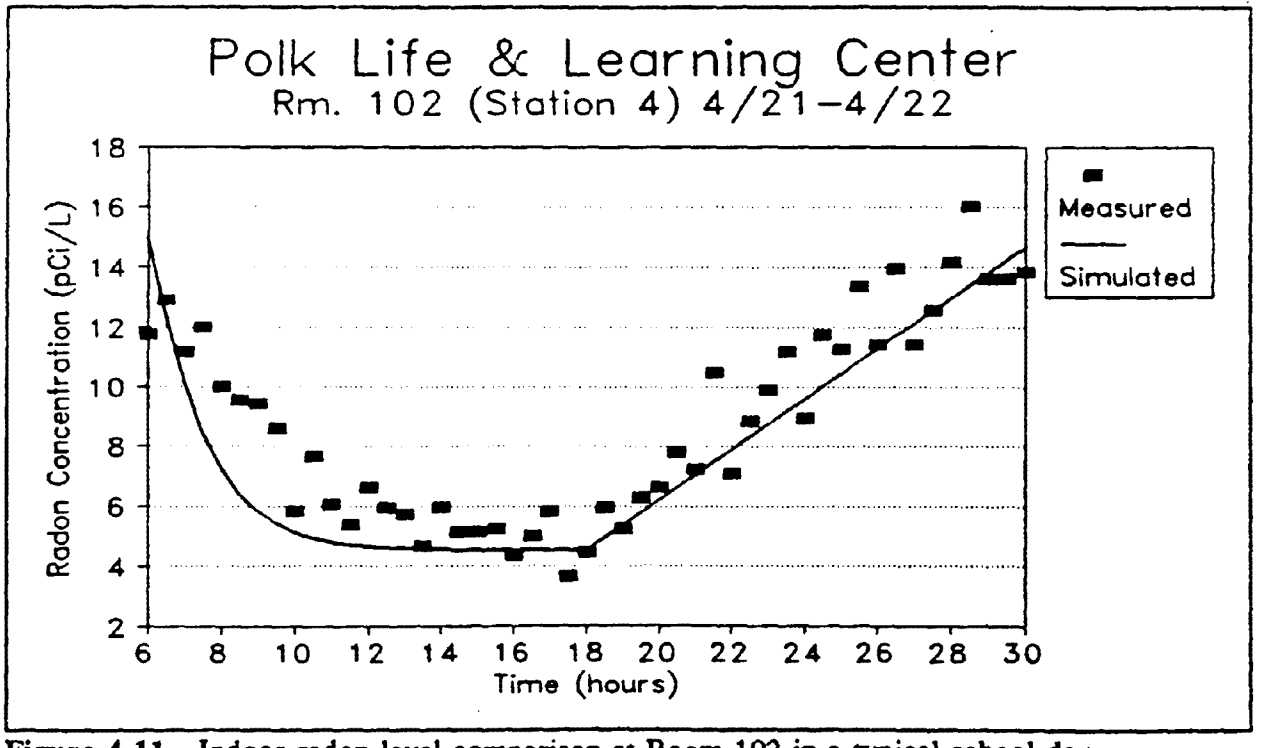

Figure 4-11. Indoor radon level comparison at Room 102 in a typical school day.

5 PARAMETRIC STUDY

5.1 Introduction

Following the validation simulation of the large building, parametric studies are presented in this Chapter, using the building configuration of Polk Life and Learning Center. It should be noted that airflow rates of supply and return are the same as those used in the seven-hour simulations.

5.2 Varying Outdoor Airflow

Figures 5-1 and 5-2 show indoor radon levels as a function of outdoor airflow for different ambient radon levels when the A/C is on. Indoor radon levels decrease with increasing outdoor airflow through the air distribution system. When small amounts of outdoor airflow are introduced, indoor radon levels increase dramatically because of less dilution. However, when a large amount of outdoor airflow is introduced, for instance, above 1500 cfm for this building, there is little effect to reduce indoor radon levels. The optimal outdoor airflow can be determined from the present simulation, based on building configuration, air conditioning system and radon levels of ambient and soil conditions.

On other hand, as long as the ambient radon level is lower than the indoor level, adding more outdoor air can dilute indoor radon. However, when the ambient radon level is higher than indoor levels, outdoor airflow will have the opposite effect; that is, the indoor radon level will increase. This is an important consideration in determining action levels for indoor radon.

5.3 Varying Ambient Radon Level

Figures 5-3 and 5-4 show the indoor radon level varying with ambient conditions for different amounts of outdoor airflow through the air distribution system. Indoor radon levels at different zones tend to increase linearly with increased ambient radon levels. Consequently, even though a large amount of airflow is introduced, the indoor radon level may remain high when the ambient radon level is high because fresh air dilution is not effective.

5.4 Varying Soil Radium Content

Figures 5-5 and 5-6 show the effect of soil radium concentration at different outdoor airflow rates and ambient radon levels. The indoor radon level increases when radium concentration in the soil increases, and vice versa. From this investigation, the relationship between indoor radon and soil radium content seems linear for a certain amount of airflow. The audiology room has the highest indoor radon level in the building based on the simulation results.

5.5 Closure

Through limited parametric studies, it is clear that outdoor airflow is the main factor in reducing indoor radon level by dilution. Since bringing in more outdoor air will lead to a penalty of

higher energy demand, any radon reduction strategies should be evaluated to optimize both good indoor air quality and energy consumption. It is worth noting that since no experimental data are available to validate the parametric studies for pressure difference between indoor and outdoor, the advection effect in parametric studies is not shown in the present report.

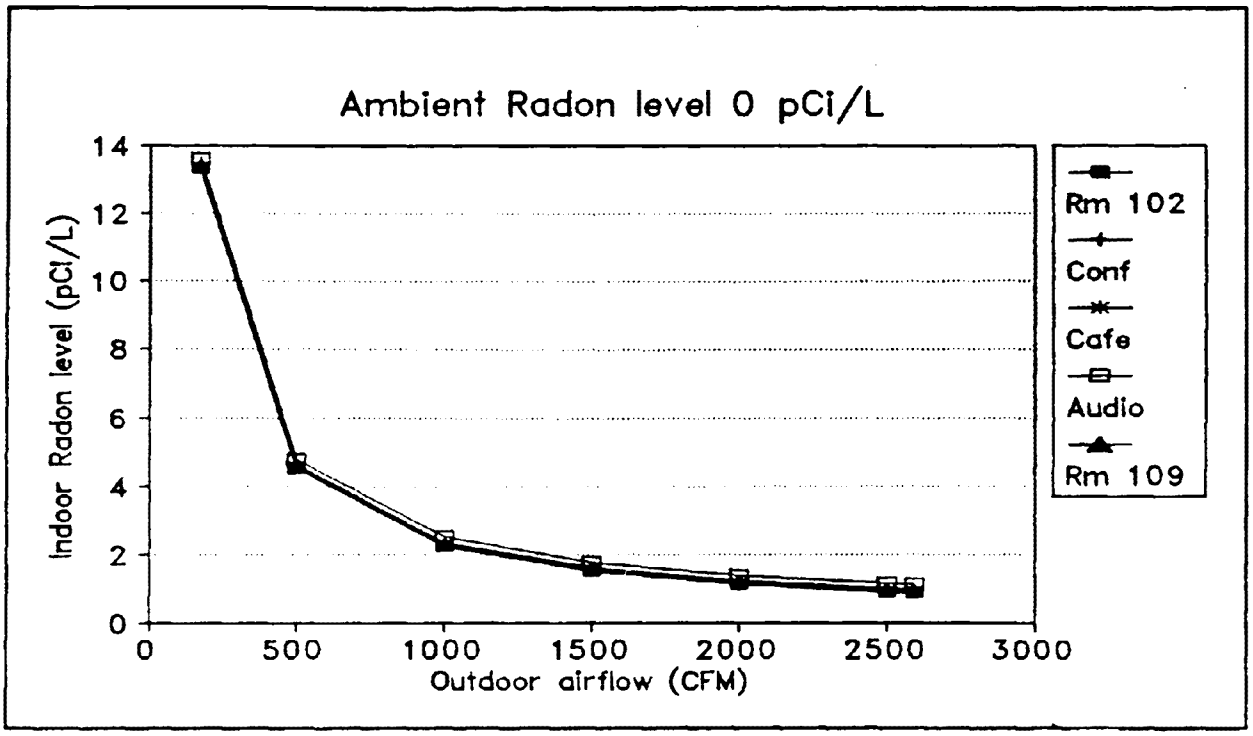

Figure 5-1. Effect of outdoor airflow on indoor radon levels (0 pCi/L ambient).

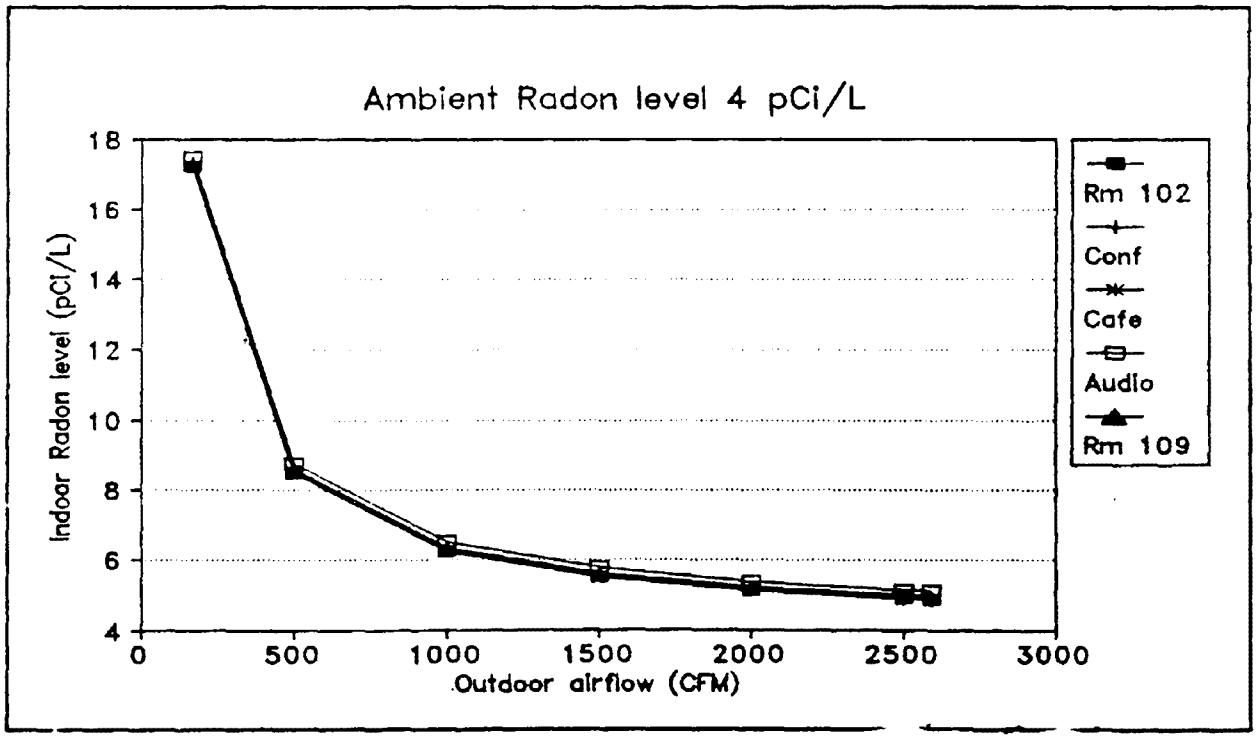

Figure 5-2. Effect of outdoor airflow on indoor radon levels (4 pCi/L ambient).

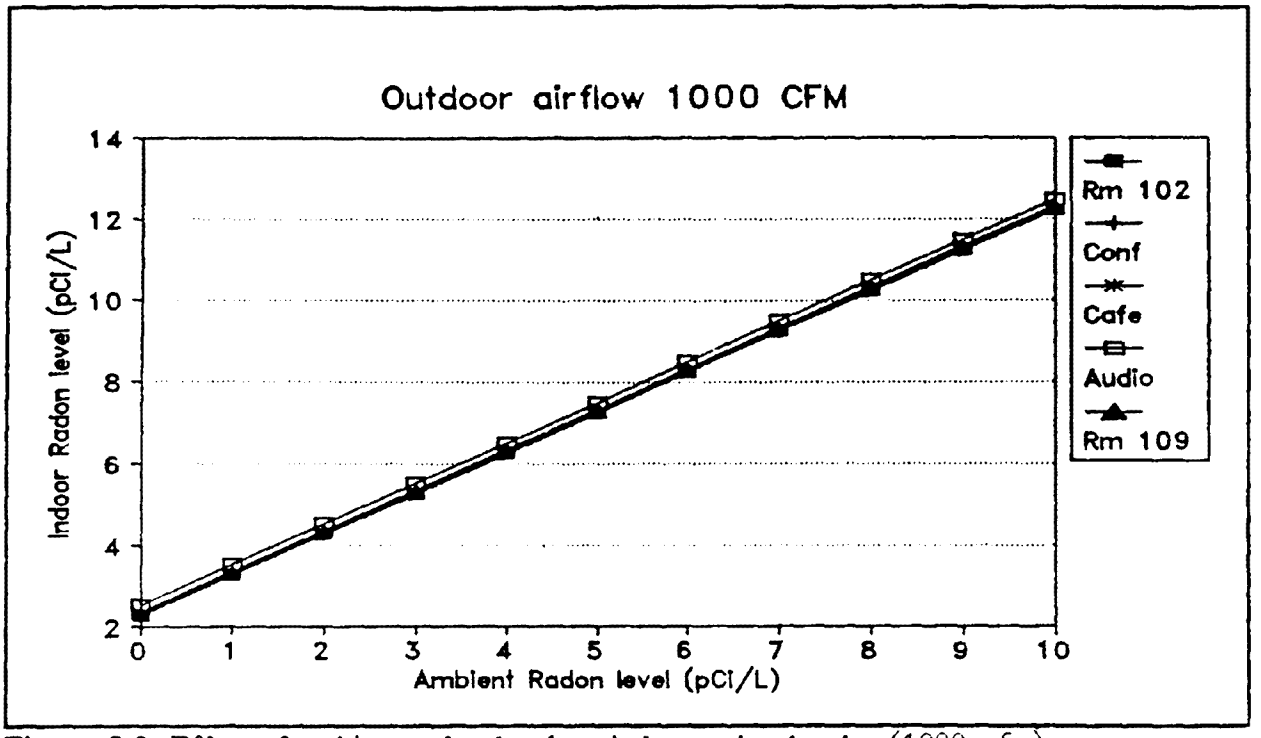

Figure 5-3. Effect of ambient radon level on indoor radon levels. (1000 cfm).

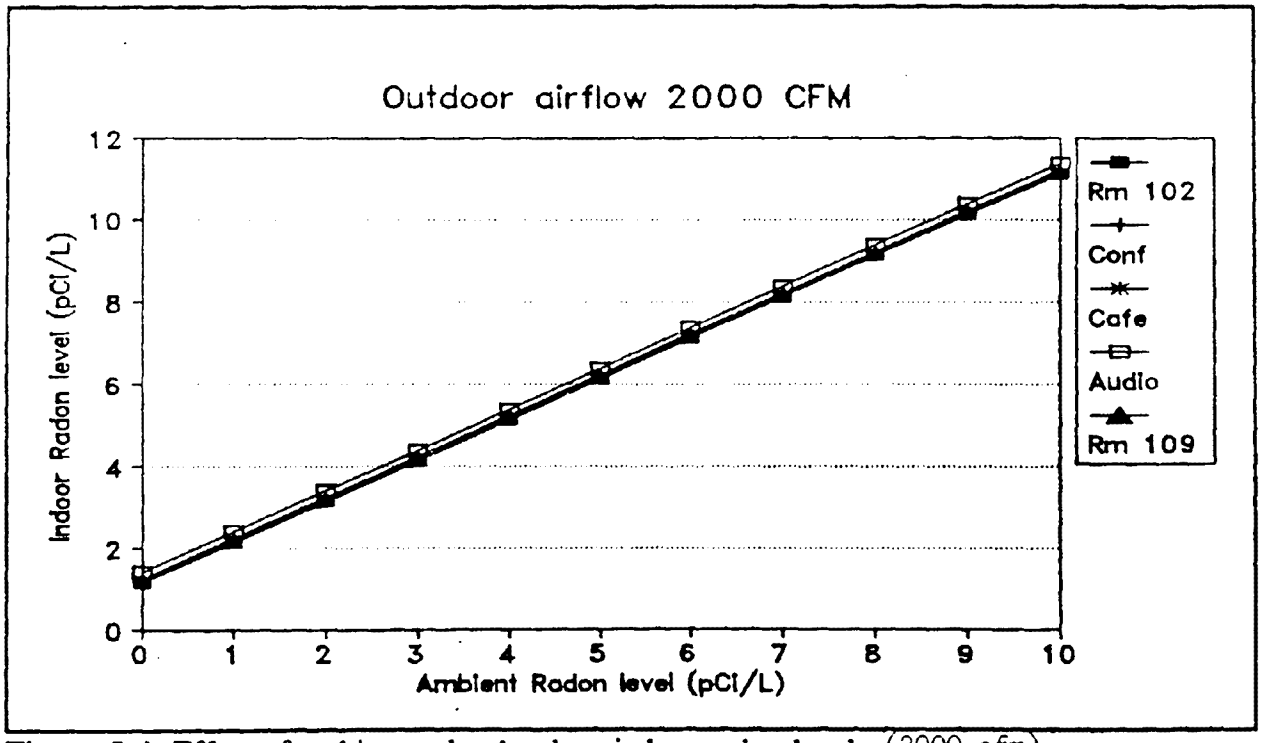

Figure 5-4. Effect of ambient radon level on indoor radon levels (2000 cfm).

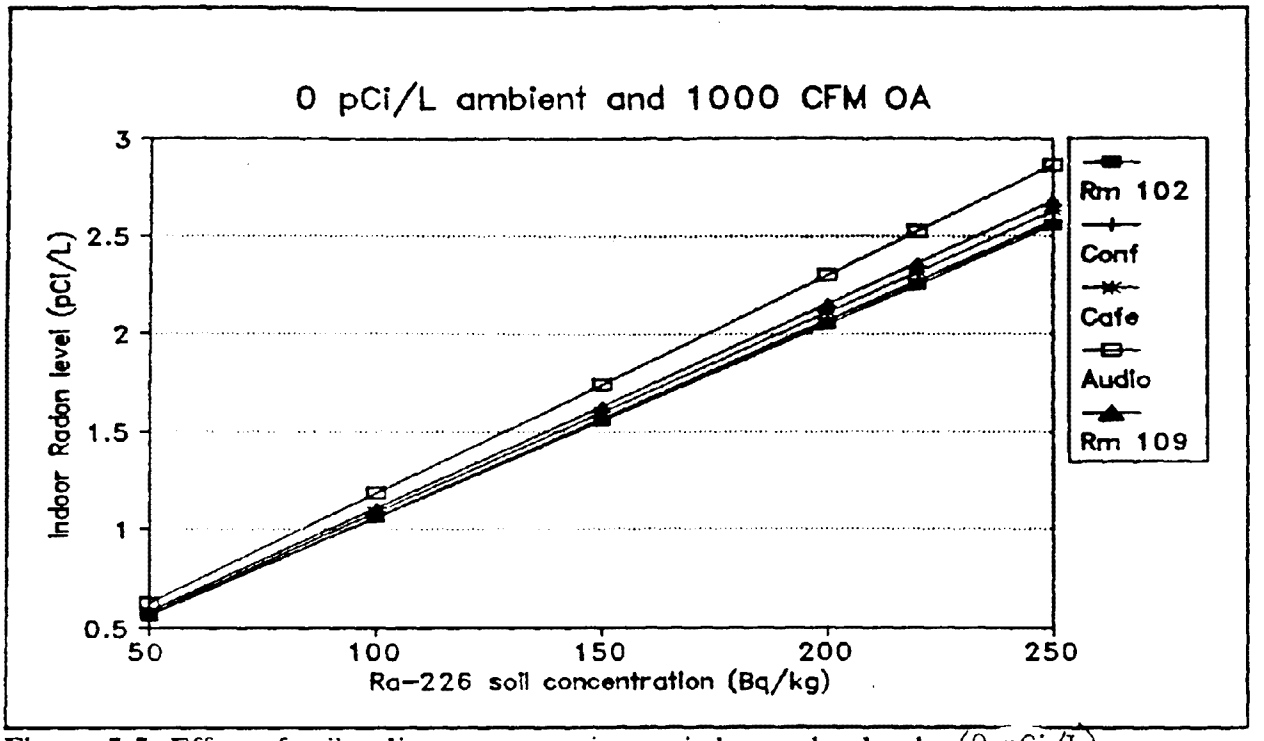

Figure 5-5. Effect of soil radium concentration on indoor radon levels (0 pCi/L).

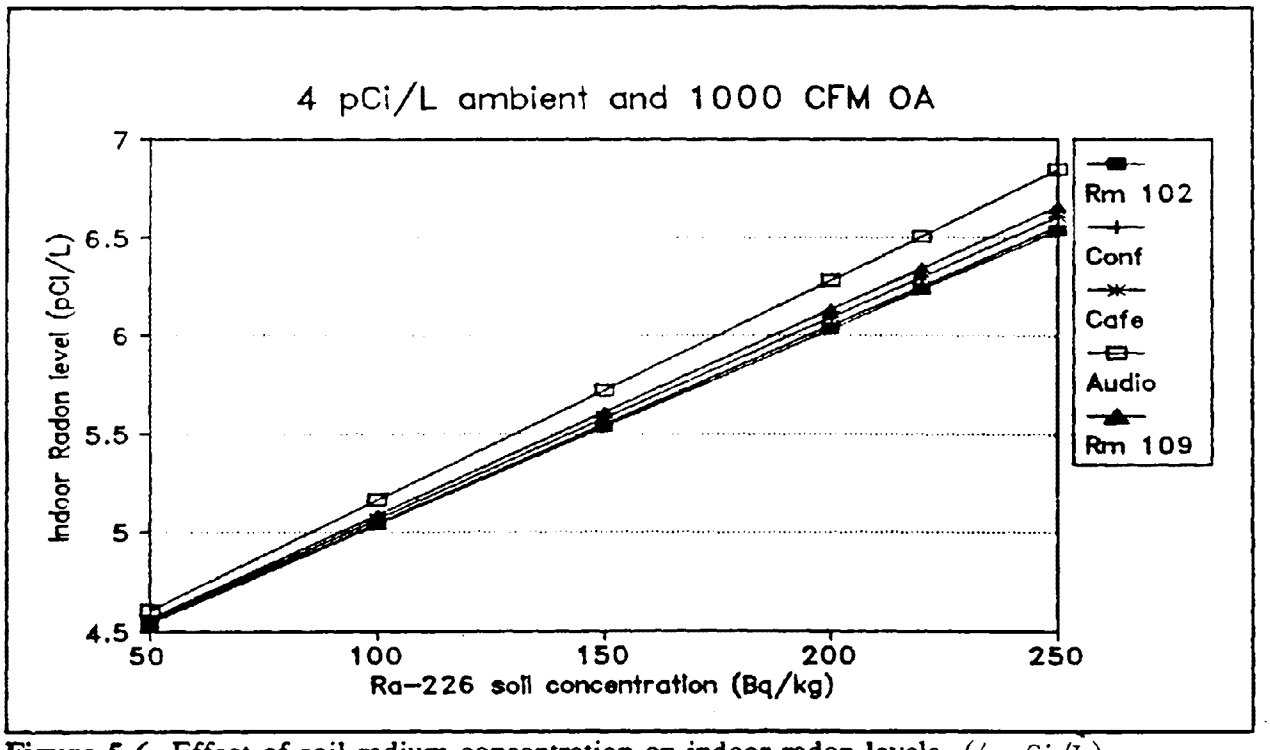

Figure 5-6. Effect of soil radium concentration on indoor radon levels (4 pCi/L).

6 CONCLUSION

Multizone airflow, indoor pressure and radon concentration, and radon entry rate from the slab are simulated in a large building, Polk Life and Learning Center at Bartow, Florida. Excellent comparison between the testing or design and predicted airflow rates at the terminals have been obtained in the HVAC system simulation. Reasonable comparison of the indoor radon level between simulation and measurement is obtained for both cases, seven-hour calibration and one typical day validation. Following the validation, parametric studies show that outdoor air flow rate is main factor affecting the indoor radon concentration. However, ambient radon level and soil radium content affect indoor radon level directly. Linear relationship is shown between indoor and outdoor radon levels. One can conclude that the best strategy for the present problem to reduce indoor radon concentration is to increase the rate of outdoor airflow.

In order to reduce the indoor radon level, the amount of outdoor airflow can play an important role in radon reduction strategy. However, a penalty of increasing energy demand will occur in order to cool more outdoor air. Therefore, an optimal condition should be determined to use minimum energy while maintaining good indoor air quality.

Topics for further investigation

- Ventilation efficiency
- Less energy consumption by introducing more fresh air
- Exhaust fan effect
- Other indoor pollutant
- Zone energy and moisture simulation
- Cost analysis
- Soli depressurization system analysis
- Pressure difference between indoor and outdoor

Caveats:

It is crucial to note that the nature of the work performed here is an exploratory one primarily to establish the potential of using models to analyze large buildings and to identify the essential areas for experiment and simulation to compliment each other in providing an accurate, yet cost efficient strategy to study radon in large buildings. This objective was substantially achieved through a preliminary simulation of airflows and pressures in a school building monitored by the US EPA and the SRI. Since only a limited set of experimental data were available, several assumptions were made to successfully complete the simulations. The results presented in this report, should therefore, be viewed in light of the assumptions stated and applied only to the specific problem analyzed. The result should in no way be construed to represent generalizations for large-buildings. The present report concludes with a list of areas that need further attention.

7 REFERENCES

Cheng, P., "Geothermal Heat Transfer," Handbook of Heat Transfer Applications, 2nd Ed., Edited by Rohsenow, W. M., Hartnett, J. P. & Ganic, E. N., McGraw-Hill Inc., New York, 1985

FSEC 3.0, Florida Software for Enervironment Computation - User's Manual, Version 3.0, FSEC-GP-47-92, Florida Solar Energy Center, Cape Canaveral, Florida, 1992

Rogers, V. C. & Nielson, K. K., "Multiphase Radon generation and Transport in Porous Materials," Health Physics, Vol. 60, No. 6, pp. 807-815, 1991

Tyson, J. L., Fairey, P. W. & Withers, C. R., "Elevated Radon Levels in Ambient Air," Indoor Air Quality and Climate Helsinki, Finland, June 27 - July 2, 1993

Walton, G., AIRNET User Manual, NISTIR 89-4072, US Department of Commerce, Washington DC, 1989

Yuan, Y. C. & Roberts, C. J., "Numerical Investigation of Radon Transport through a Porous Medium," Transaction of American Nuclear Society, Vol. 38, pp. 108-110, 1981

TECHNICAL REPORT DATA
(Please read Instructions on the reverse before completi

1. REPORT NO.	2.	3.
EPA-600/R-96-116		

4. TITLE AND SUBTITLE	5. REPORT DATE
Large Building HVAC Simulation	September 1996
	6. PERFORMING ORGANIZATION CODE
7. AUTHOR(S)	8. PERFORMING ORGANIZATION REPORT NO.
Lixing Gu, Muthusamy V. Swami, and Vailoor Vasanth	FSEC-CR-616-93
9. PERFORMING ORGANIZATION NAME AND ADDRESS	10. PROGRAM ELEMENT NO.
Florida Solar Energy Center 300 State Road 401 Cape Canaveral, Florida 32920	11. CONTRACT/GRANT NO. 68-D0-0097 Work Assignment 3-12
12. SPONSORING AGENCY NAME AND ADDRESS	13. TYPE OF REPORT AND PERIOD COVERED
EPA, Office of Research and Development **Air Pollution Prevention and Control Division** **Research Triangle Park, NC 27711**	Final report; 3/92-4/93 14. SPONSORING AGENCY CODE **EPA/600/13**

15. SUPPLEMENTARY NOTES APPCD project officer is Marc Y. Menetrez, Mail Drop 54, 919/541-7981.

16. ABSTRACT The report discusses the monitoring and collection of data relating to indoor pressures and radon concentrations under several test conditions in a large school building in Bartow, Florida. The Florida Solar Energy Center (FSEC) used an integrated computational software, FSEC 3.0, to simulate heating, ventilation, and air-conditioning system and multizone airflows, indoor pressures, radon transport in the soil, and slab and indoor radon levels in the large building. The simulation was validated by measured data. A limited parametric study shows the influence of outdoor airflow, ambient radon level, and soil radium content on indoor radon levels.

17. KEY WORDS AND DOCUMENT ANALYSIS

a. DESCRIPTORS		b. IDENTIFIERS/OPEN ENDED TERMS	c. COSATI Field/Group
Pollution	Soils	Pollution Control	13B 08G, 08M
Radon	Slabs	Stationary Sources	07B 13C
Heating	Radium	Heating, Ventilation, and Air-conditioning Systems	13H, 13A
Ventilation			
Air Conditioning			
School Buildings			13M, 05I

18. DISTRIBUTION STATEMENT	19. SECURITY CLASS *(This Report)*	21. NO. OF PAGES
Release to Public	**Unclassified**	42
	20. SECURITY CLASS *(This page)*	22. PRICE
	Unclassified	

EPA Form 2220-1 (9-73)